soil systems

MDPI

Pedogenic Processes in a *Posidonia oceanica* Mat

Nerea Piñeiro-Juncal [1,2,*], **Carmen Leiva-Dueñas [2]**, **Oscar Serrano [3]**, **Miguel Ángel Mateo [2,3]** **and Antonio Martínez-Cortízas [1]**

[1] EcoPast (GI-1553), Departamento de Edafoloxía e Química Agrícola, Facultade de Bioloxía, Universidade de Santiago de Compostela, Santiago de Compostela, 15782 A Coruña, Spain; antonio.martinez.cortizas@usc.es

[2] Centre d'Estudis Avançats de Blanes, Consejo Superior de Investigaciones Científicas, Blanes, 17300 Girona, Spain; cleiva@ceab.csic.es (C.L.-D.); mateo@ceab.csic.es (M.Á.M.)

[3] School of Science and Centre for Marine Ecosystems Research, Edith Cowan University, 6027 Joondalup, WA, Australia; o.serranogras@ecu.edu.au

* Correspondence: nerea.pineiro.juncal@rai.usc.es

check for updates

Abstract: Scientists studying seagrasses typically refer to their substratum as sediment, but recently researchers have begun to refer to it as a soil. However, the logistics of sampling underwater substrata and the fragility of these ecosystems challenge their study using pedological methods. Previous studies have reported geochemical processes within the rhizosphere that are compatible with pedogenesis. Seagrass substratum accumulated over the Recent Holocene and can reach several meters in thickness, but studies about deeper layers are scarce. This study is a first attempt to find sound evidence of vertical structuring in *Posidonia oceanica* deposits to serve as a basis for more detailed pedological studies. A principal component analysis on X-Ray Fluorescence-elemental composition, carbonate content and organic matter content data along a 475 cm core was able to identify four main physico-chemical signals: humification, accumulation of carbonates, texture and organic matter depletion. The results revealed a highly structured deposit undergoing pedogenetical processes characteristic of soils rather than a mere accumulation of sediments. Further research is required to properly describe the substratum underneath seagrass meadows, decide between the sediment or soil nature for seagrass substrata, and for the eventual inclusion of seagrass substrata in soil classifications and the mapping of seagrass soil resources.

Keywords: seagrass; marine sediments; subaqueous soils; geochemistry; X-ray fluorescence

1. Introduction

Subaqueous soils were first recognized in the second edition of the Soil Taxonomy (ST) [1]. The World Reference Base (WRB) has acknowledged soils to occur underwater as well, to a maximum depth of 2 m [2]. Until recently, the substrate below marine phanerogams has been studied as sediment by marine biologists and chemists. The recent interest from a soil science perspective has resulted in a few publications in which seagrass substrates are envisioned as soils [3–6], triggering discussion about their classification as sediment or soil [7]. Regardless of the terminology used, the plant/substrate interactions lead to physico-chemical changes that dramatically modify the texture [8,9] and composition [10–13], increase organic matter content (OM) [14], microbial populations and diversity [15–18], while changing redox potential [19]. All these processes are typical of pedogenetical evolution in continental soils. Although this topic may seem trivial, soils are considered important resources worldwide, supporting food and agriculture, biodiversity and the preservation of cultural heritage, among others, and are protected by environmental laws accordingly.

Seagrasses are a polyphyletic group of marine angiosperms which can be found in coastal waters of all continents except Antarctica [20]. One of the seagrass species that largely alters the substrate

where it grows is *Posidonia oceanica* [12,21,22], an endemic species from the Mediterranean Sea that inhabits coastal areas up to 48 m water depth [23]. *Posidonia oceanica* increases sedimentation through lowering hydrodynamic energy and by the direct trapping of suspended particles by the canopy [24]. The increased sedimentation, together with the accumulation of large amounts of belowground tissues from the seagrass itself, results in the formation of well-structured deposits known as mats [25]. The anoxic environment prevailing within the mat, owing to a high OM content and low oxygen availability, and the refractory nature of the seagrass detritus [26], hamper the rapid mineralization cycles [27] and consequently favor the accumulation of organic carbon that contributes to climate change mitigation [28]. The mats underneath *P. oceanica* meadows have also been found to serve as a habitat for reef fish species [29], contribute to coastal protection against erosion [30], act as filters and sinks for pollutants [31] and constitute security vaults of archaeological heritage [32]. Furthermore, like peatlands, they provide long and chronologically well-ordered records of environmental change and human activities in coastal areas [31,33,34]. Nowadays, the most extended methods for seagrass ecosystems' regression and impacts' evaluation are measurements of surface cover, shoot density and plant biomass [35,36]. No monitoring is being carried out of the seagrass deposit itself or of "dead meadows" deposits where the plant cover has been lost but the deposit remains, undergoing different degrees of erosion. The classification of these deposits as soils will contribute to promote their conservation under specific soil regulations schemes, as well as their mapping and monitoring, and to raise public awareness about their fragility and sensitivity to coastal management policies. The logistics required to investigate these ecosystems make sampling arduous and impede the use of common pedological methodologies, such as field horizon description. Furthermore, like peatlands, deposits under seagrasses take thousands of years to accumulate [21,37], and the anthropic pressure has strongly diminished their extension in the Mediterranean Sea [38]. European regulations have been implemented to help protect these ecosystems, but seem to only be slowing the plant cover loss [35]. Due to the fragility of the ecosystem, minimizing the impact of sampling is fundamental.

Although biogeochemical processes within the rhizosphere of *P. oceanica* have been profusely investigated [39], biogeochemical studies of the layers below it are rare. Some of the few studies characterizing *P. oceanica* deposits below the rhizosphere come from a meadow in Portlligat bay (NE Spain) where long mat cores have been used as environmental records [31,34], to characterize the deposit [5] and to study the long-term carbon cycle associated to the ecosystem [26,40]. The results from these studies point to an active physico-chemical environment, above and below the rhizosphere, far from a mere accumulation of sediments. The present study is intended as the next step to understand the long-term processes leading to the formation and evolution of *P. oceanica* deposit, looking for evidence of horizonation or vertical structuring before considering larger scale pedogenetical studies. To this end, we analyzed the elemental composition (using X-ray fluorescence; XRF), as well as the carbonate and OM contents along a 475 cm-long *P. oceanica* core encompassing the last 4000 years and contextualize it within the available information about the Portlligat seagrass mat, aiming at understanding the formation processes.

2. Material and Methods

2.1. Study Area and Sampling Methods

The core studied was collected in 2000 in Portlligat Bay (42°17′32″ N, 3°7′28″ E; NE Spain), a shallow embayment (<10 m depth) connected to the sea by a 213 m-wide opening to the NE (Figure 1). *P. oceanica* meadows cover 41% of the bay area, and sandy bioclastic patches and rocky bottom are dispersed throughout [41]. The bay receives eventual terrestrial inputs from a creek in its NW shore, modulated by the Mediterranean climate of the area. Precipitation mainly occurs from October to December, with values ranging between 200 and 1300 mm (average range for the period 1950–2016, meteorological station of Roses, Servei Meteorològic de Catalunya). Portlligat bay is embedded within Roses Gulf, which originated 400 million years ago with the Pyrenees, belonging to

a migmatitic complex that consists of an association of sillimanite schists, granitoids, quartz-gabbros and pegmatites [42].

　　A 475 cm-long, 8.5 cm in inner diameter core was recovered from the seagrass mat at around 3 m water depth using a floating drilling platform with a self-powered rotopercutor hammer. The sampling details are further described elsewhere [5].
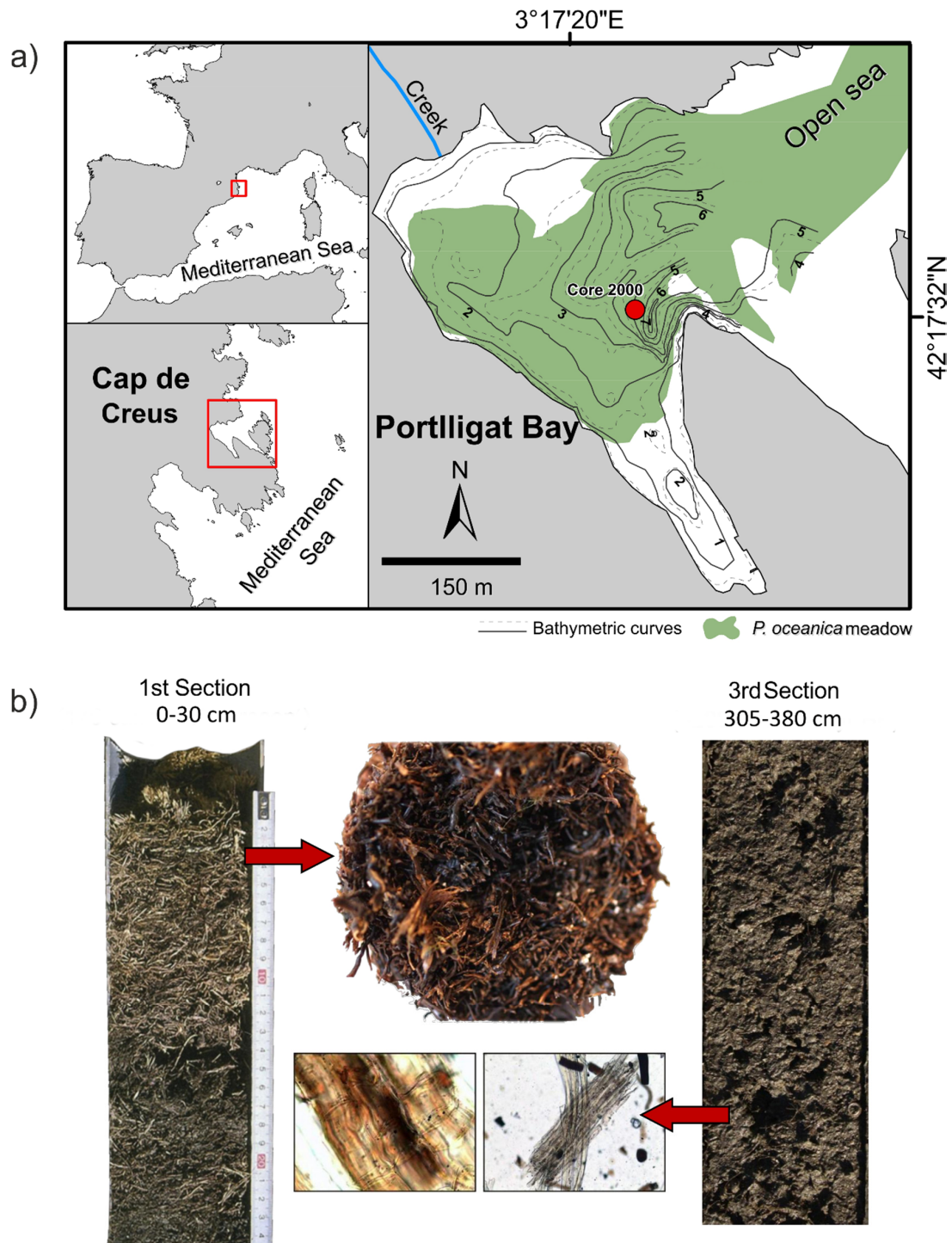

Figure 1. (**a**) Coring site of the *P. oceanica* soil core in Portlligat Bay (Girona, Spain); (**b**) detail of the upper and lower sections of the core, where plant fibers can be found. Modified from Leiva-Dueñas (2018) [43].

2.2. Geochemical Analysis

The core was cut into 1 cm slices which were oven-dried at 70 °C until constant weight. The bulk samples were ground to obtain homogeneous powder. Samples were analyzed by X-ray fluorescence (EMMA-XRF) at the Infrastructure Network for the Support of Research and Technological Development (Universidade de Santiago de Compostela), to obtain the concentrations of the following elements: sulfur, bromine, silicon, potassium, phosphorus, chlorine, aluminum, rubidium, strontium, calcium, chromium, magnesium, arsenic, zirconium, lead, iron and titanium [44,45]. The equipment was calibrated using standard reference materials. The quantification limits were 2 g·kg^{-1} for S, 1 g·kg^{-1} for Cl and Mg, 0.5 g·kg^{-1} for Ca and K, 0.1 g·kg^{-1} for Ti and P, 0.05 g·kg^{-1} for Si and Al, 0.01 g·kg^{-1} for Fe, 15 µg·g^{-1} for Cr, 1 µg·g^{-1} for Pb and As, 0.5 µg·g^{-1} for Br, 0.3 µg·g^{-1} for Rb and Sr, and 0.2 µg·g^{-1} for Zr. Coarse (>1 mm) and fine (<1 mm) organic matter (COM and FOM, respectively); the carbonate contents used in this study were previously published; and analyses procedures and details can be found elsewhere [5].

2.3. Statistical Methods:

The correlation of the elements is analyzed by principal component analysis (PCA) using *psych* package 1.8.12 [46] in R software version 3.4.4 [47]. Data were previously transformed by centered log ratio (CLR) to avoid spurious relationships related to compositional data [48]. A varimax rotation was used to maximize the variance of the variables in the components. All components with eigenvalues >1 were considered. Change phases (CP) in each principal component scores record were determined by change-point modelling, CPQtR1.0.3 [49].

3. Results

3.1. Organic Matter, Carbonates and Elemental Composition

At first sight, most of the variables studied started with a maxima or minima at the top of the core, then increased or decreased sharply or gradually along the first meter, and finally stabilized down the core (Figure 2). A notable interruption of this trend occurred at around 300 cm for all the minor and major elements, and for most of the trace elements (with some exceptions or to a lesser extent). Another disruptive event in this general trend was observed at around 450 cm.

Among the major and minor elements determined (Si, Al, Fe, Ti, Ca, K, Mg, P, S and Cl), concentrations of Ca and Si were higher (ranging between 10–20%) than Al and Cl (3–4%), Fe, Mg, S and K (1–2%) and Ti and P (0.10–0.15%). Among the trace elements (Rb, Sr, Zr, Cr, As, Pb and Br), Sr showed the highest concentration (around 1000 µg·g^{-1}), followed by Zr, Mn and Br (100–180 µg·g^{-1}), Cr and Rb (30–75 µg·g^{-1}), and Pb and As (10–20 µg·g^{-1}). Carbonate content (m, 45.4 ± 11%) was higher than OM content (3.1% ± 2.8% FOM and 6% ± 9.4% COM; Figure 2) along the core. However, the carbonate content within the top 110 cm of the mat was lower (28.3% ± 4.8%) than from cm 110 to cm 475 (50.5% ± 5.9%). FOM content was higher in the first 30 cm (10.8% ± 3.4%), and COM content was higher within the top 50 cm (23.5% ± 16.9%) compared to the rest of the core (2.5% ± 1.3% and 3.3% ± 2.3%, respectively).
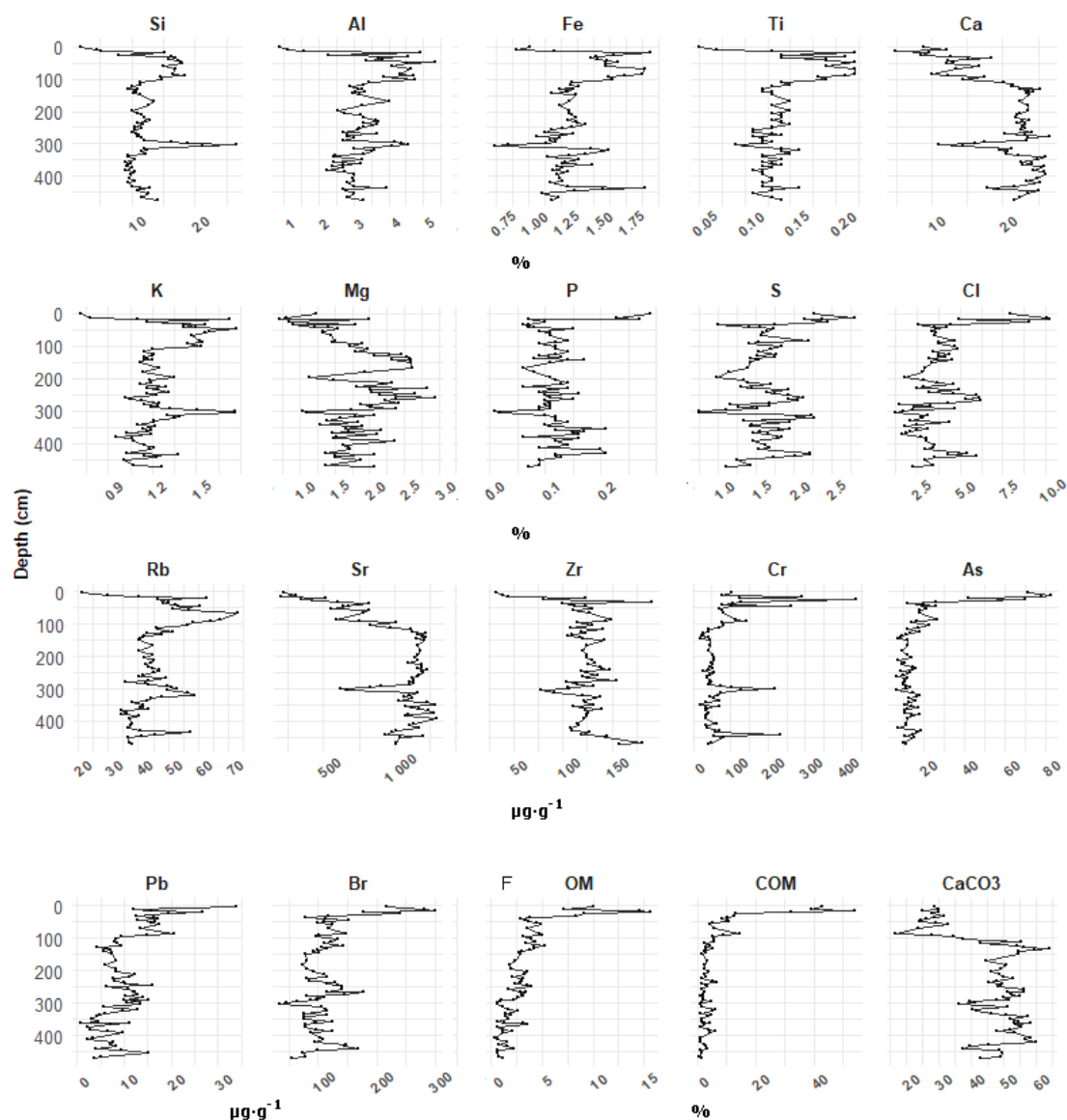
Figure 2. Major and minor elements (Si, Al, Fe, Ti, Ca, K, Mg, P, S and Cl), trace elements (Rb, Sr, Zr, Cr, As, Pb and Br), fine organic matter (FOM), coarse organic matter (COM) and carbonate concentration along the *P. oceanica* core studied.

3.2. Geochemical Signals

The PCA yielded four principal components, accounting for 83% of the total variance (Table 1). All variables show high communalities (> 0.5). For each component, several change points (CPs) were found: two for PC1, two for PC2, two for PC3 and six for PC4 (Figure 3). CPs indicate the probability of a change of phase in the PC scores, but do not necessarily encompass the whole phase of change (e.g., CP1.1 between 16 and 25 cm and observed inflexion trend in the scores at 35 cm, Figure 3).

The first component (PC1) explains 32.9% of the total variance, showing high positive loadings (>0.7) for Si, K, Al and Rb, moderate positive loadings (0.4–0.6) for Ti and Zr, while high negative loadings are shown by S, P, Br (<−0.7) and moderate negative loadings by Cl and As (−0.4 to −0.7; Table 1, Figure 4). The component scores decrease from the top of the core until 35 cm (CP1.1; Figure 3) and remain stable below this depth, with the exception of a local increase around 300 cm (CP1.2; Figure 3).

Table 1. Loadings of chemical elements, coarse organic matter (COM), fine organic matter (FOM) and carbonates for each component as yielded by the principal components analysis (PCA). Com: communality (total variance of each variable explained by the extracted components), Var. %: percentage of variance accounted for by each component; Ac. Var. %: cumulative variance. Loadings > 0.35 in bold.

|	PC1	PC2	PC3	PC4	Com
Si	**0.94**	0.15	0.08	−0.11	0.93
K	**0.88**	−0.01	0.04	−0.18	0.81
Al	**0.88**	0.24	0.20	−0.01	0.87
S	**−0.85**	−0.15	0.03	−0.21	0.79
Rb	**0.83**	−0.09	0.22	−0.01	0.75
P	**−0.83**	0.14	0.14	−0.01	0.72
Br	**−0.81**	**−0.42**	−0.07	0.14	0.85
Cl	**−0.67**	**−0.37**	−0.25	0.16	0.66
Sr	0.18	**0.91**	0.11	−0.28	0.95
Ca	−0.01	**0.88**	−0.02	**−0.36**	0.90
COM	−0.15	**−0.87**	0.06	−0.00	0.78
Mg	−0.02	**0.84**	−0.08	−0.02	0.71
Cr	0.24	**−0.82**	−0.27	−0.09	0.82
As	**−0.42**	**−0.82**	−0.03	−0.04	0.85
CaCO$_3$	0.19	**0.76**	−0.13	**−0.53**	0.91
Zr	**0.46**	**0.70**	0.26	−0.16	0.79
Fe	0.13	−0.01	**0.92**	0.03	0.87
Ti	**0.61**	−0.01	**0.70**	0.13	0.88
Pb	0.14	**−0.40**	**−0.50**	**0.62**	0.81
FOM	−0.13	−0.12	0.14	**0.92**	0.89
Var. %	32.9	30.5	9.9	9.5	
Ac. Var. %	32.9	63.4	73.3	82. 8	
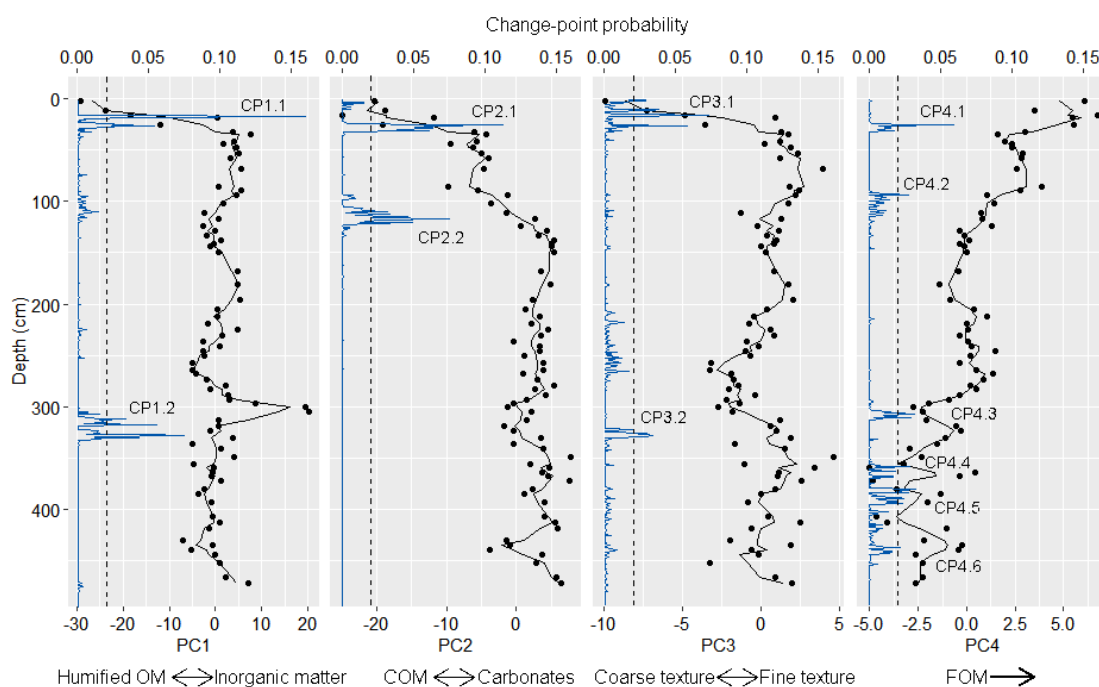
Figure 3. Depth records of principal components (PCs) scores, dots; moving average of PCs scores, grey line. Change point probability, blue line; limit to consider a change point (0.02), black dashed line.

The second principal component (PC2) accounts for 30.5% of the total variance, with high positive loadings for Sr, Ca, Mg, CaCO$_3$ and Zr, high negative loadings for COM, As and Cr, and moderate to

low negative loadings for Pb, Br and Cl (Table 1, Figure 4). The scores increase sharply from the top of the core until 35 cm (CP2.1; Figure 3), followed by stable values between 35 cm and 100 cm and an increase from 100 cm to 130 cm (CP2.2, Figure 3). Values are relatively constant below 130 cm depth.

The third principal component (PC3) explains 9.9% of the variance, and it is mainly related to Fe and Ti, with high positive loadings, and to Pb with a moderate negative loading (Table 1, Figure 4). The scores increase sharply within the upper 30 cm (CP3.1, Figure 3), but show low variation below 30 cm, except for a shift to negative values between 200 cm and 300 cm (starting at 330, CP3.2, Figure 3).

The fourth principal component (PC4) accounts for 9.5% of the variance with positive loadings for FOM (high) and Pb (moderate) and negative, moderate to low, loadings for $CaCO_3$ and Ca (Table 1, Figure 4). The record of scores shows a decreasing trend from the surface to the bottom, with a slight shift to more negative values below 300 cm (Figure 3). This is the component with the highest number of change points, most of them of low probability and located at the bottom part of the core (6; Figure 3).
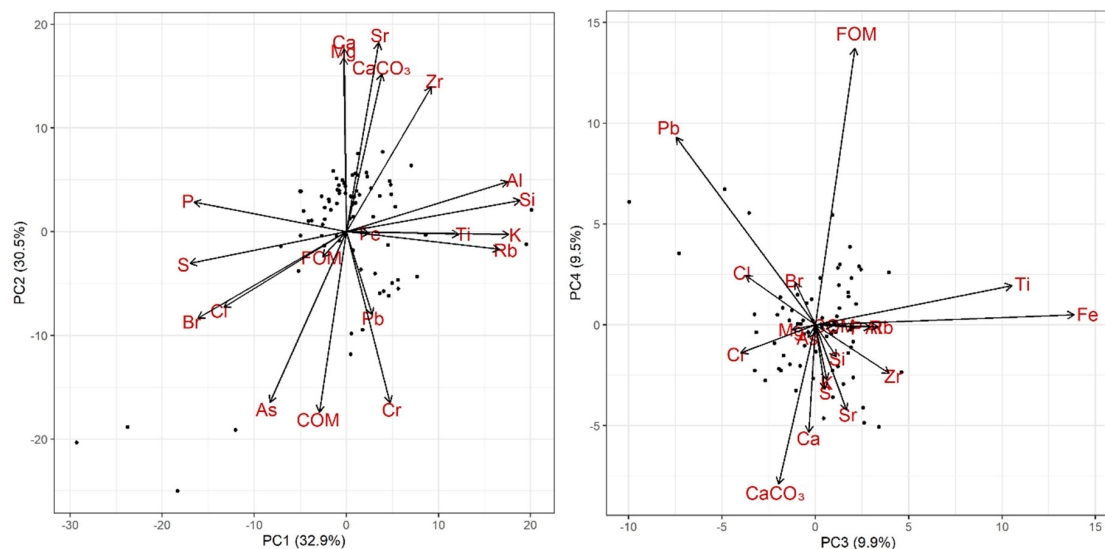

Figure 4. PCA loadings (black arrows). The black dots represent the samples distribution according to their scores in the plotted principal components.

4. Discussion

Although information about the biogeochemistry of the substrate of the Portlligat meadow is scarce, it is by far the best-studied seagrass deposit below 50 cm from the sediment top, as it has been used as a source of paleo-environmental information [31,33,34,43,50]. The average thickness of the deposit has been estimated to be 4.5 m, accumulated in the last 6000 years [41]. The material used in this study was a peaty-like dark brown to grey material, releasing an intense smell of sulfide, which contains *P. oceanica* macro remains along the entire core length [5]. The mineralization of OM has been studied through pyrolysis techniques finding a selective preservation of p-hydroxybenzoic acids and the degradation of carbohydrates and syringyl lignin down core [26,51]. Microbial metabolism is expected to follow a chain of electron acceptors (O_2, NO_{3-}, Mn, Fe, SO_4^{-2} and CO_2) being the aerobic activity dominant in the area of influence of the rhizosphere due to the diffusion of O_2 through the roots [40].

Our results, supported by the information discussed above, indicate a clear vertical structure in the mat, mainly determined by the dynamics of OM mineralization. The mineralization process is very likely controlled by the presence/absence of roots, which influence microbial metabolism by O_2 diffusion and the recalcitrance of *P. oceanica* debris, leading to two mineralization phases above and below the rhizosphere. Due to the decrease in OM content with depth, the carbonate content increases. The two horizons that can be determined by the ST (histic and calcic) coincide with the two main processes found, the humification of OM and the accumulation of carbonates (negative PC1 and positive PC2).

Only one horizon has been determined following the WRB, related with high to medium accumulation of OM, where humification is captured by the first principal component, and the deposited material was classified as calcic due to the high concentration of carbonates. Furthermore, two more components were identified in the PCA. The third principal component is related to soil texture and the fourth to OM depletion. Several metallic elements were found to covary with OM. The interpretation of this covariance is unclear and further research is recommended to better understand the metals' behavior and interpret their accumulation.

4.1. Organic VS Inorganic Matter Accumulation

In the first component of the PCA (PC1), the opposite relationship between elements typical of mineral matter (Si, Al, K, Rb, Ti and Zr) and biophyle (S and P) [52] plus organically bound elements (Cl and Br; Table 1), suggests a mass balance between inorganic and organic matter content within the *P. oceanica* mat. Chlorine and Br are indicators of marine OM [52–55], as they are known to enzymatically bind to OM during humification (e.g., halogenation of aliphatic and aromatic compounds) [56–58]. Neither COM nor FOM show high loadings in this component. Coarse OM is composed by *P. oceanica* macro-debris (i.e., sheaths, roots and rhizomes) barely degraded in our core [5], and it is the major part of the total OM (59 ± 14.5%). The fact that COM is not correlated with PC1 supports the hypothesis that the OM in the negative scores of this component represents the highly humified fraction, instead of the total OM, which includes the rhizosphere and macro seagrass debris. However, the humified OM would necessarily belong to one or both of the two OM fractions (COM and FOM), and very likely to both, as their contents decrease from the top to 35 cm (Figure 2) at the same time that a decrease in the humified OM is detected (increase in PC1 scores with depth, Figure 3). The fact that COM and FOM do not have high loadings in PC1 may be due to the small proportion of samples reflecting this process in the core (9% of the samples), with S, P, Br and Cl being quickly depleted and not following COM and FOM variations in the remaining record (91% of the samples).

The first principal component scores distribution shows high negative values in the upper 35 cm (CP1.1, Figure 3), indicating a high content of humified OM in accordance with our interpretation, a characteristic inherent to a soil epipedon. Based on the age–depth model for this core reported by Serrano et al. (2012), the humification processes may seem to have prevailed during the last ≈300 cal. years BP after burial. A study of the molecular composition of the OM on the same core found that the main changes in organic compounds of COM occured between 200 and 400 cal. years BP [26]. Despite the long-term stability of OM within *P. oceanica* mats, which is related to the recalcitrance of seagrass OM and the anoxic conditions prevailing within the soil [59,60], the O_2 pumped by the roots within the top of the core [19,61] results in high aerobic microbial activity [40] and the rapid decomposition of the labile fractions of the OM [26,51], explaining the depletion of OM in the top of the core (Figure 2) and coinciding with the elevated humification signal of PC1. Changes in PC1 scores below the upper 35 cm are minor, except for a maximum at 300 cm (CP1.2). These small changes likely reflect past changes in the proportion of mineral and organic inputs to the soil of the meadow. The main change observed is a 15-fold excursion to positive values at 300 cm depth (Figure 3), concurring with a high erosion phase in the bay catchment led by an increase in flooding events [62] and human activity, which is in agreement with environmental paleoreconstructions of the area [34,43].

4.2. Accumulation of Carbonates

The second principal component clusters Sr, Ca, Mg, carbonates and Zr with positive loadings, against COM, Cr, As and, to some extent, Pb (Table 1), pointing to a balance between carbonate accumulation and OM. The rapid decomposition of COM and FOM within the top 35 cm resulted in an enrichment of carbonate content, followed by further OM mineralization and enrichment of carbonates, Sr, Ca, Mg and Zr, until 130 cm where both OM and carbonate contents stabilized.

Biologically mediated precipitation by calcifying organisms is the most plausible source of carbonates to seagrass deposits at our study site, stimulated by the augmented water pH resulting from

intense photosynthetic activity [5,12,63,64] and the low hydrodynamic energy environment prevailing within the bay [65]. The correlation of Sr with Ca is also indicative of biogenic carbonates [52]. However, a recent study suggests that allochthonous carbonate sources could be the main origin of carbonates in seagrass meadows [66] and in our core Ca also covaries with Zr and Mg, elements associated to lithogenic sources, so this source cannot be discarded. The carbonate concentration in our core is lower than the average carbonate concentration reported for both the top 10 cm and top meter of *P. oceanica* deposits (28 and 122 mg·cm^{-3}, respectively) [12], which may be explained by the lack of carbonate materials in the Portlligat catchment [42].

The lower concentration of carbonates in the top layers has been observed before for seagrass mats [12]. This may be due to a dilution effect by the largest OM abundance in the top sections of the substrate (due to the presence of the rhizomes and roots of the living plant). The correlation between COM and metal elements can reflect the biological process of metal accumulation or sorption after burial [67,68]. However, the increase in As and Pb accumulation in the top-most of the core can be related to atmospheric metal pollution [31]. Scores from PC2 showed negative values in the upper part of the core, increasing downcore in two steps to positive values at 35 cm and 150 cm (CP2.1 and CP2.2; Figure 3). These two change phases can be a result of different OM mineralization stages. The first one coincides with the humification trend detected in PC1, during which the coarse detritus is physically degraded and seagrass labile compounds, such as fatty acids and polysaccharides, are consumed faster [26,51]. The second decay step is slower (CP2.2, Figure 3; ≈1050 years after burial) because the remaining COM fraction, mainly composed of *P. oceanica* debris, is now enriched in more recalcitrant compounds such as phenols and aromatics [26]. Furthermore, the microbial community below the rhizosphere shifts to a predominant anaerobic metabolism [40], which is slower and less efficient than aerobic metabolism [69]. Both the OM composition and the sediment environmental conditions can explain the second, slower OM mineralization phase.

4.3. Enrichment in Fine Soil Particles

The third principal component accounts for the distribution of Fe and Ti, and it is likely related to changes in terrestrial runoff and/or dust deposition [52]. Iron and Titanium are usually enriched in the clay fraction of continental soils and sediments [70,71]. Alternatively, Fe in solution can precipitate at the sediment water interface, due to the alkaline pH of the seawater [72] and the oxygen pumped by *P. oceanica* roots [19,61], but this does not explain Ti accumulation, as it is mostly hosted in highly resistant minerals (such as rutile and titanite), therefore supporting the former hypothesis.

The third principal component scores show fairly constant values below 35 cm, with the exception of relatively lower values between 200 cm and 300 cm (CP3.2), suggesting a coarser grain size composition (Figure 3). It is interesting to note that this decrease in fine mineral particles is coeval with the peak in inorganic mineral content (PC1 scores, CP1.2, Figure 3), reinforcing the occurrence of an intense 'terrestrial event' already discussed elsewhere [34,43]. Again, a high accumulation of plant remains in the upper part of the soil and could account for the large decrease in Fe and Ti concentrations (CP3.1).

The negative correlation found between Pb and Fe and Ti in this component can be related to historical processes (e.g., increased Pb fluxes from human activities in the last 300 years, [73]; coinciding with the decrease of Fe and Ti by OM dilution), or may be pointing to different sources (e.g., land erosion vs. atmospheric deposition). Thus, the increased Pb concentrations may be responding to regional or global processes [31] and not to soil geochemistry. Further research would be needed to clarify this process.

4.4. Fine Organic Matter (FOM)

The fourth principal component scores tend to decrease with depth throughout the core, which is likely linked to OM mineralization (Figure 3). FOM concentration would be the result of a balance between outputs due to microbial mineralization and inputs from the fragmentation of COM.

The negative covariation with the carbonate content may reflect the effect of FOM in diluting carbonate concentration, as discussed above for PC1 and PC2.

It is not clear whether the correlation between FOM and Pb concentrations is related to geochemical processes. However, the formation of organometallic complexes [67,68] during diagenesis seems to be the most likely explanation.

According to the change point modeling, this component is the noisiest, especially at the bottom, although all the changes show low probability. The high score values until CP4.1 coincide with the low values of CP1 (Figure 3), most likely linked to the initial fast degradation of OM detected in both PC1 and PC2. CP4.2 co-occurs with the end of the second OM degradation phase (see Section 4.2, Figure 3).

4.5. Soil Classification

Although a proper soil classification is out of the scope of this study, a preliminary classification is proposed, aiming at triggering a debate around the eventual inclusion of seagrass deposits in the soil classification.

4.5.1. Soil Taxonomy (ST)

A first requirement is determining whether the studied soil is composed by mineral or organic material (as specified in the Soil Taxonomy). As it is always saturated with water (thus more than the 30 days per year required), the OM content criterion depends on clay content. Serrano et al. (2012) reported that mud (clay + silt) content in the same core was <60% at any depth, and therefore the clay content would be lower than 60%. If the material contains no clay, then the OM limit for being classified as organic material is 12% and, in our core, this condition is met down to 44 cm. As seagrass meadows promote the deposition of fine grain-size material [8,9], the presence of clay is enhanced, and the minimum OM content for organic soil is calculated as: (clay (%) × 0.1) + 12. As an exercise, we made the conservative assumption that the mud content reported by Serrano et al. (2012) was all clay (even though it surely includes silt); the organic material in the studied soil pedon would reach, uninterruptedly, 34 cm from the core top.

The OM humification process identified in the upper part of the core (PC1, see Section 4.1) indicates the presence of an active epipedon. The depth of the epipedon would determine its classification. If we follow the ST classification key, the surface horizon can be classified as histic, i.e., an organic soil that is water-saturated for more than 30 days a year. Although oxic microenvironments may occur in the rhizosphere of seagrass [74–76], their extent and persistence would depend on the O_2 diffusion from the roots, which ceases at night and varies seasonally [19], matching the requirement for the material to be under reducing conditions for some time during a normal year. It consists of organic material that is 20 to 40 cm thick. The epipedon studied would reach 34 to 44 cm depth, concurring with the change from organic to mineral material. Below that depth, the remaining deposit can be classified as a calcic horizon: it is more than 15 cm thick, contains more than 15% carbonate and does not meet the requirements for a petrocalcic horizon.

The classification of the soil depends on the actual depth of the histic horizon. Assuming that there is no clay or that the clay content is <20%, the soil can be classified as Haplofibrist, as the fibric material predominates in the histic horizon. Otherwise, the soil can be classified as Humaquept: it has aquic conditions and a histic epipedon.

4.5.2. World Reference Base (WRB)

In accordance with the WRB, subaqueous soils can only be covered by a water layer of no more than 2 m at low spring tides [2]. The pedon we have studied does not meet this requirement, but shallower parts of the meadow at Portlligat Bay do.

To be considered organic material, the deposit must have above 20% soil organic carbon. There is no data available for organic carbon content in our core, but Fourqurean et al. (2012) published equations to convert OM (obtained by Loss in Ignition; LOI) to organic carbon (Corg) in seagrass deposits:

$$\%LOI < 0.2 \; \% \; Corg = 0.40*\%LOI\text{-}0.21 \; r^2\text{: } 0.87$$

$$\%LOI > 0.2 \; \% \; Corg = 0.43*\%LOI\text{-}0.33 \; r^2\text{: } 0.96$$

Using these formulas, we can determine that the organic carbon content is higher than 20% in only three samples (at 1, 12 and 14 cm depth), with the mineral fraction being the dominant one along the core. The whole core can be considered as calcaric material as it contains >2% of $CaCO_3$ at all depths and fluvic material consistent with a stratified marine deposit.

In disagreement with the ST, with the WRB the upper part of the soil cannot be classified as a histic horizon. It would be classified as either a mollic or umbric horizon, as it is thick, dark-colored and has a ≥0.6% of organic carbon, although a final classification would require further laboratory analysis (we do not have the base saturation of the exchange complex). With the data available, the soil can tentatively be classified as a calcic Fluvisol, as it contains fluvic material and is rich in carbonates.

5. Conclusions

The vertical differentiation observed would strongly support *P. oceanica* mats being not just a mere accumulation of sediments, but a highly structured deposit with a particular functioning and characteristics, more consistent with the definition of soils. *Posidonia oceanica* rhizosphere seems to greatly influence the chemistry of the deposit, as seen for other seagrasses [39], as the main changes in the processes occur in the top-most part of the core. Organic matter mineralization shows two phases, very likely within and below the rhizosphere. The horizons preliminarily identified may correspond to the sections where these two phases occur, showing the ability of current soil classification keys to describe the chemical structuration of this deposit by routine analysis. The slow OM degradation is not a unique feature of *P. oceanica,* as most seagrasses are known to promote long-term OM storage [10,37], suggesting that similar structuration and processes may be common in other seagrass deposits around the world. Further research is required to properly describe and classify the substratum underneath seagrass meadows, which can contribute to deciding between the sediment or soil nature of seagrass substrata, the eventual inclusion of seagrass substrata in soil classifications and the mapping of seagrass soil resources. This effort may be urgent, as seagrass meadows are declining worldwide, and their inclusion as soils may boost conservation efforts.

References

1. Soil Survey Staff. *Soil Taxonomy: A Basic System of Soil Classification for Making and Interpreting Soil Surveys*; Natural Resourse Conservation Service, USA Department Agriculture: Washington, DC, USA, 1999.
2. IUSS Working Group. World reference base for soil resources 2014. In *International Soil Classification System for Naming Soils and Creating Legends for Soil Maps*; World Soil Resources Reports No. 106; Cambridge University Press: Cambridge, UK, 2015; pp. 1–191. [CrossRef]

3. Nóbrega, G.N.; Romero, D.J.; Otero, X.L.; Ferreira, T.O. Pedological studies of subaqueous soils as a contribution to the protection of seagrass meadows in Brazil. *Revista Brasileira Ciência Solo* **2018**, *42*, 1–12. [CrossRef]

4. Nóbrega, G.N. Subaqueous soils of the Brazilian seagrass meadows: Biogeochemistry, genesis, and classification. Ph.D. Thesis, University of São Paulo, São Paulo, Brasil, 2017.

5. Serrano, O.; Mateo, M.A.; Renom, P.; Julià, R. Characterization of soils beneath a *Posidonia oceanica* meadow. *Geoderma* **2012**, *185*, 26–36. [CrossRef]

6. Bradley, M.P.; Stolt, M.H. Subaqueous soil-landscape relationships in a Rhode Island estuary. *Soil Sci. Soc. Am. J.* **2003**, *67*, 1487–1495. [CrossRef]

7. Kristensen, E.; Rabenhorst, M.C. Do marine rooted plants grow in sediment or soil? A critical appraisal on definitions, methodology and communication. *Earth Sci. Rev.* **2015**, *145*, 1–8. [CrossRef]

8. Rueda, J.L.; Salas, C.; Marina, P. Seasonal variation in a deep subtidal *Zostera marina* L. bed in southern Spain (western Mediterranean Sea). *Bot. Mar.* **2008**, *51*, 92–102. [CrossRef]

9. Van Katwijk, M.M.; Bos, A.R.; Hermus, D.C.R.; Suykerbuyk, W. Sediment modification by seagrass beds: Muddification and sandification induced by plant cover and environmental conditions. *Estuar. Coast. Shelf Sci.* **2010**, *89*, 175–181. [CrossRef]

10. Fourqurean, J.W.; Duarte, C.M.; Kennedy, H.; Marbà, N.; Holmer, M.; Mateo, M.A.; Apostolaki, E.T.; Kendrick, G.A.; Krause-Jensen, D.; McGlathery, K.J.; et al. Seagrass ecosystems as a globally significant carbon stock. *Nat. Geosci.* **2012**, *5*, 505–509. [CrossRef]

11. Kennedy, H.; Gacia, E.; Kennedy, D.P.; Papadimitriou, S.; Duarte, C.M. Organic carbon sources to SE Asian coastal sediments. *Estuar. Coast. Shelf Sci.* **2004**, *60*, 59–68. [CrossRef]

12. Mazarrasa, I.; Marbà, N.; Lovelock, C.E.; Serrano, O.; Lavery, P.S.; Fourqurean, J.W.; Kennedy, H.; Mateo, M.A.; Krause-Jensen, D.; Steven, A.D.; et al. Seagrass meadows as a globally significant carbonate reservoir. *Biogeosciences* **2015**, *12*, 4993–5003. [CrossRef]

13. Smit, A.J.; Brearley, A.; Hyndes, G.A.; Lavery, P.S.; Walker, D.I. Carbon and nitrogen stable isotope analysis of an *Amphibolis griffithii* seagrass bed. *Estuar. Coast. Shelf Sci.* **2005**, *65*, 545–556. [CrossRef]

14. Duarte, C.M.; Middelburg, J.J.; Caraco, N. Major role of marine vegetation on the oceanic carbon cycle. *Biogeosciences* **2005**, *2*, 1–8. [CrossRef]

15. Cifuentes, A.; Antón, J.; Benlloch, S.; Donnelly, A.; Herbert, R.A.; Rodríguez-Valera, F. Prokaryotic diversity in *Zostera noltii* colonized marine sediments. *Appl. Environ. Microbiol.* **2000**, *66*, 1715–1719. [CrossRef] [PubMed]

16. Danovaro, R. Detritus-bacteria-meiofauna interactions in a seagrass bed (*Posidonia oceanica*) of the NW Mediterranean. *Mar. Biol.* **1996**, *127*, 1–13. [CrossRef]

17. Jones, W.B.; Cifuentes, L.A.; Kaldy, J.E. Stable carbon isotope evidence for coupling between sedimentary bacteria and seagrasses in a sub-tropical lagoon. *Mar. Ecol. Prog. Ser.* **2003**, *255*, 15–25. [CrossRef]

18. Lopez, N.I.; Duarte, C.M.; Vallespinos, F.; Romero, J.; Alcoverro, T. Bacterial activity in NW Mediterranean seagrass (*Posodonia oceania*) sediments. *J. Exp. Mar. Bio. Ecol.* **1995**, *187*, 39–49. [CrossRef]

19. Borum, J.; Sand-Jensen, K.; Binzer, T.; Pedersen, O.; Greve, T.M. Oxygen movement in seagrasses. In *Seagrasses: Biology, Ecology and Conservation*; Springer: Dordrecht, The Netherlands, 2006; pp. 255–270.

20. Hartog, C.; Den Kuo, J. Taxonomy and biogeography of seagrasses. In *Seagrasses: Biology, Ecology and Conservation*; Springer: Dordrecht, The Netherlands, 2006; pp. 1–23.

21. Serrano, O.; Lavery, P.S.; López-Merino, L.; Ballesteros, E.; Mateo, M.A. Location and associated carbon storage of erosional escarpments of seagrass *Posidonia* mats. *Front. Mar. Sci.* **2016**, *3*, 1–7. [CrossRef]

22. Trevathan-Tackett, S.M.; Seymour, J.R.; Nielsen, D.A.; Macreadie, P.I.; Jeffries, T.C.; Sanderman, J.; Baldock, J.; Howes, J.M.; Steven, A.D.L.; Ralph, P.J. Sediment anoxia limits microbial-driven seagrass carbon remineralization under warming conditions. *FEMS Microbiol. Ecol.* **2017**, *93*, 1–15. [CrossRef]

23. Augier, H.; Boudouresque, C. *Premières Observations sur l'herbier de Posidonies et le Détritique Côtier de l'île du Levant (Méditérranée, France), à L'aide du Sous-Marin Griffon de la Marine Nationale*; Travaux scientifiques du Parc National de Port-Cros: Hyères, France, 1979; pp. 141–153.

24. Koch, E.W.; Ackerman, J.D.; Verduin, J.; van Keulen, M. Fluid dynamics in seagrass ecology-from molecules to ecosystems. In *Seagrasses: Biology, Ecology and Conservation*; Springer: Dordrecht, The Netherlands, 2006; pp. 193–225.

25. Boudouresque, C.; Meinesz, A. Découverte de l'herbier de posidonie. In *Parc National de Port-Cros*; Podidonie, G.I.S., Ed.; Parc Naturel Régional de la Corse: Corte, France, 1982.

26. Kaal, J.; Serrano, O.; Nierop, K.G.J.; Schellekens, J.; Martínez Cortizas, A.; Mateo, M.-Á. Molecular composition of plant parts and sediment organic matter in a Mediterranean seagrass (*Posidonia oceanica*) mat. *Aquat. Bot.* **2016**, *133*, 50–61. [CrossRef]

27. Canfield, D.E. Factors influencing organic-carbon preservation in marine-sediments. *Chem. Geol.* **1994**, *114*, 315–329. [CrossRef]

28. Duarte, C.M.; Losada, I.J.; Hendriks, I.E.; Mazarrasa, I.; Marbà, N. The role of coastal plant communities for climate change mitigation and adaptation. *Nat. Clim. Chang.* **2013**, *3*, 961–968. [CrossRef]

29. Serrano, O.; Serrano, E.; Inostroza, K.; Lavery, P.S.; Mateo, M.A.; Ballesteros, E. Seagrass meadows provide 3D Habitat for Reef Fish. *Front. Mar. Sci.* **2017**, *4*, 3–5. [CrossRef]

30. Ondiviela, B.; Losada, I.J.; Lara, J.L.; Maza, M.; Galván, C.; Bouma, T.J.; van Belzen, J. The role of seagrasses in coastal protection in a changing climate. *Coast. Eng.* **2014**, *87*, 158–168. [CrossRef]

31. Serrano, O.; Mateo, M.; Dueñas-Bohórquez, A.; Renom, P.; López-Sáez, J.A.; Martínez Cortizas, A. The *Posidonia oceanica* marine sedimentary record: A Holocene archive of heavy metal pollution. *Sci. Total Environ.* **2011**, *409*, 4831–4840. [CrossRef] [PubMed]

32. Krause-Jensen, D.; Serrano, O.; Apostolaki, E.T.; Gregory, D.J.; Duarte, C.M. Seagrass sedimentary deposits as security vaults and time capsules of the human past. *Ambio* **2019**, *48*, 325–335. [CrossRef]

33. López-Sáez, J.A.; López-Merino, L.; Mateo, M.Á.; Serrano, Ó.; Pérez-Díaz, S.; Serrano, L. Palaeoecological potential of the marine organic deposits of *Posidonia oceanica*: A case study in the NE Iberian Peninsula. *Palaeogeogr. Palaeoclimatol. Palaeoecol.* **2009**, *271*, 215–224. [CrossRef]

34. López-Merino, L.; Colás-Ruiz, N.R.; Adame, M.F.; Serrano, O.; Martínez Cortizas, A.; Mateo, M.A. A six thousand-year record of climate and land-use change from Mediterranean seagrass mats. *J. Ecol.* **2017**, 1–12. [CrossRef]

35. De los Santos, C.B.; Krause-Jensen, D.; Alcoverro, T.; Marbà, N.; Duarte, C.M.; van Katwijk, M.M.; Pérez, M.; Romero, J.; Sánchez-Lizaso, L.J.; Roca, G.; et al. Recent trend reversal for declining European seagrass meadows. *Nat. Commun.* **2019**, *10*, 1–8. [CrossRef]

36. Zieman, J.C.; Fourqurean, J.W.; Frankovich, T.A. Seagrass die-off in Florida Bay: Long-term trends in abundance and growth of turtle grass. *Thalassia testudinum. Estuaries* **1999**, *22*, 460–470. [CrossRef]

37. Lavery, P.S.; Mateo, M.Á.; Serrano, O.; Rozaimi, M. Variability in the carbon storage of seagrass habitats and its implications for global estimates of Blue Carbon ecosystem service. *PLoS ONE* **2013**, *8*, e73748. [CrossRef]

38. Telesca, L.; Belluscio, A.; Criscoli, A.; Ardizzone, G.; Apostolaki, E.T.; Fraschetti, S.; Gristina, M.; Knittweis, L.; Martin, C.S. Seagrass meadows (*Posidonia oceanica*) distribution and trajectories of change. *Sci. Rep.* **2015**, *5*, 1–14. [CrossRef]

39. Marbà, N.; Holmer, M.; Gacia, E.; Barrón, C. Seagrass beds and coastal biogeochemistry. In *Seagrasses: Biology, Ecology and Conservation*; Springer: Dordrecht, The Netherlands, 2006; pp. 133–155.

40. Piñeiro-Juncal, N.; Mateo, M.Á.; Holmer, M.; Martínez-Cortizas, A. Potential microbial functional activity along a *Posidonia oceanica* soil profile. *Aquat. Microb. Ecol.* **2018**, *81*, 189–200. [CrossRef]

41. Lo Iacono, C.; Mateo, M.A.; Grácia, E.; Guasch, L.; Carbonell, R.; Serrano, L.; Serrano, O.; Dañobeitia, J. Very high-resolution seismo-acoustic imaging of seagrass meadows (Mediterranean Sea): Implications for carbon sink estimates. *Geophys. Res. Lett.* **2008**, *35*, 1–5. [CrossRef]

42. Institut Geològic de Catalunya. Geologic map Alt Emporda (1:50000). 2006. Available online: https://www.icgc.cat/en/Public-Administration-and-Enterprises/Downloads/Geological-and-geothematic-cartography/Geological-cartography/Geological-map-1-50-000/Regional-geological-map-of-Catalonia-1-50-000 (accessed on 16 January 2020).

43. Leiva-Dueñas, C.; López-Merino, L.; Serrano, O.; Martínez Cortizas, A.; Mateo, M.A. Millennial-scale trends and controls in *Posidonia oceanica* (L. Delile) ecosystem productivity. *Glob. Planet Chang.* **2018**, *169*, 92–104. [CrossRef]

44. Cheburkin, A.K.; Shotyk, W. An Energy-dispersive miniprobe multielement analyzer (EMMA) for direct analysis of Pb and other trace elements in peats. *Fresenius J. Anal. Chem.* **1996**, *354*, 688–691. [CrossRef]

45. Weiss, D.; Shotyk, W.; Cheburkin, A.K.; Gloor, M. Determination of Pb in the ash fraction of plants and peats using the energy-dispersive miniprobe multielement analyser (EMMA). *Analyst* **1998**, *123*, 2097–2102. [CrossRef]

46. Revelle, W. *Psych: Procedures for Personality and Psychological Research*; Northwestern University: Evanston, IL, USA, 2017.

47. R Development Core Team. *R: A Language and Environment for Statistical Computing*; R Core Team: Vienna, Austria, 2013.

48. Aitchison, J. The statistical analysis of compositional data. *J. R. Stat. Soc. Ser. B* **1982**, *44*, 139–177. [CrossRef]

49. Gallagher, K.; Bodin, T.; Sambridge, M.; Weiss, D.; Kylander, M.; Large, D. Inference of abrupt changes in noisy geochemical records using transdimensional changepoint models. *Earth Planet Sci. Lett.* **2011**, *311*, 182–194. [CrossRef]

50. Serrano, O.; Martínez-Cortizas, A.; Mateo, M.A.; Biester, H.; Bindler, R. Millennial scale impact on the marine biogeochemical cycle of mercury from early mining on the Iberian Peninsula. *Global Biogeochem. Cycles* **2013**, *27*, 21–30. [CrossRef]

51. Piñeiro-Juncal, N.; Kaal, J.; Fornazier Moreira, J.C.; Martínez-Cortizas, A.; Rodrigues Lambais, M.; Otero, X.L.; Mateo, M.A. Cover loss of Posidonia oceanica meadows causes organic matter remineralization and shifts in the prokaryotic communities in the underlying soil. in preparation.

52. Rothwell, R.G.; Croudace, I.W. Twenty years of XRF core scanning marine sediments: What do geochemical proxies tell us? In *Micro-XRF Studies of Sediment Cores: Applications of a Non-Destructive Tool for the Environmental Sciences*; Springer: Berlin/Heidelberg, Germany, 2015; pp. 25–102.

53. Dembitsky, V.M. Bromo and iodo containing alkaloids from marine microorganisms and sponges. *Russ. J. Bioorganic. Chem.* **2002**, *28*, 170–182. [CrossRef]

54. Gribble, G.W. The natural production of organobromine compounds. *Environ. Sci. Pollut. Res.* **2000**, *7*, 37–49. [CrossRef] [PubMed]

55. Ziegler, M.; Jilbert, T.; De Lange, G.J.; Lourens, L.J.; Reichart, G.J. Bromine counts from XRF scanning as an estimate of the marine organic carbon content of sediment cores. *Geochem. Geophys. Geosyst.* **2008**, *9*, 1–6. [CrossRef]

56. Leri, A.C.; Mayer, L.M.; Thornton, K.R.; Ravel, B. Bromination of marine particulate organic matter through oxidative mechanisms. *Geochim. Cosmochim. Acta.* **2014**, *142*, 53–63. [CrossRef]

57. Martínez-Cortizas, A.; Ferro-Vázquez, C.; Kaal, J.; Biester, H.; Casais, M.C.; Rodríguez, T.T.; Rodríguez Lado, L. Bromine accumulation in acidic black colluvial soils. *Geochimica Cosmochimica Acta* **2016**, *174*, 143–155. [CrossRef]

58. Myneni, S.C.B. Formation of stable chlorinated hydrocarbons in weathering plant material. *Science* **2002**, *295*, 1039–1041. [CrossRef]

59. Trevathan-Tackett, S.M.; Macreadie, P.I.; Sanderman, J.; Baldock, J.; Howes, J.M.; Ralph, P.J. A global assessment of the chemical recalcitrance of seagrass tissues: Implications for long-term carbon sequestration. *Front. Plant Sci.* **2017**, *8*, 1–18. [CrossRef]

60. Kaal, J.; Serrano, O.; del Río, J.C.; Rencoret, J. Radically different lignin composition in *Posidonia* species may link to differences in organic carbon sequestration capacity. *Org. Geochem.* **2018**. [CrossRef]

61. Holmer, M.; Duarte, C.M.; Marbà, N. Sulfur cycling and seagrass (*Posidonia oceanica*) status in carbonate sediments. *Biogeochemistry* **2003**, *66*, 223–239. [CrossRef]

62. Benito, G.; Macklin, M.G.; Zielhofer, C.; Jones, A.F.; Machado, M.J. Holocene flooding and climate change in the Mediterranean. *Catena* **2015**, *130*, 13–33. [CrossRef]

63. Canals, M.; Ballesteros, E. Production of carbonate sediments by phytobenthic communities in the Mallorca-Minorca Shelf, northwestern Mediterranean Sea. *Deep Res.* **1997**, *44*, 611–629.

64. Mateu-Vicens, G.; Brandano, M.; Gaglianone, G.; Baldassarre, A. Seagrass-meadow sedimentary facies in a mixed siliciclastic-carbonate temperate system in the Tyrrhenian Sea (Pontinian Islands, Western Mediterranean). *J. Sediment. Res.* **2012**, *82*, 451–463. [CrossRef]

65. De Falco, G.; Baroli, M.; Cucco, A.; Simeone, S. Intrabasinal conditions promoting the development of a biogenic carbonate sedimentary facies associated with the seagrass. *Posidonia oceanica. Cont. Shelf Res.* **2008**, *28*, 797–812. [CrossRef]

66. Saderne, V.; Geraldi, N.R.; Macreadie, P.I.; Maher, D.T.; Middelburg, J.J.; Serrano, O.; Almahasheer, H.; Arias-Ortiz, A.; Cusack, M.; Eyre, B.D.; et al. Role of carbonate burial in Blue Carbon budgets. *Nat. Commun.* **2019**, *10*, 1–9. [CrossRef] [PubMed]

67. Lyngby, J.E.; Brix, H. Heavy metals in eelgrass (*Zostera marina* L.) during growth and decomposition. *Hydrobiologia* **1989**, *176–177*, 189–196. [CrossRef]

68. Ragsdale, H.L.; Thorhaug, A. Trace metal cycling in the USA coastal zone: A synthesis. *Am. J. Bot.* **1980**, *67*, 1102–1112. [CrossRef]

69. Fenchel, T.; King, G.M.; Blackburn, H. *Bacterial Biogeochemistry: The Ecophysiology of Mineral Cycling*, 3rd ed.; Elsevier Academic Press: San Diego, CA, USA, 1998.

70. Schuetz, L. Atmospheric mineral dust properties and source markers. In *Paleoclimatology and Paleometeorology: Modern and Past Patterns of Global Atmospheric Transport*; Leinen, M., Sarnthein, M., Eds.; Springer: Dordrecht, The Netherlands, 1989; pp. 359–383.

71. Taboada, T.; Cortizas, A.M.; García, C.; García-Rodeja, E. Particle-size fractionation of titanium and zirconium during weathering and pedogenesis of granitic rocks in NW Spain. *Geoderma* **2006**, *131*, 218–236. [CrossRef]

72. Riley, J.P.; Chester, R. *Introduction to Marine Chemistry*; Academic Press: London, UK, 1971.

73. Martínez-Cortizas, A.; Pontevedra-Pombal, X.; Nóvoa Muñoz, J.C.; García-Rodeja, E. Four thousand years of atmospheric Pb, Cd and Zn deposition recorded by the ombrotrophic peat bog of Penido Vello (Northwestern Spain). *Water Air Soil Pollut.* **1997**, 387–403. [CrossRef]

74. Pedersen, O.; Borum, J.; Duarte, C.M.; Fortes, M.D. Oxygen dynamics in the rhizosphere of *Cymodocea rotundata*. *Mar. Ecol. Prog. Ser.* **1998**, *169*, 283–288. [CrossRef]

75. Connell, E.L.; Colmer, T.D.; Walker, D.I. Radial oxygen loss from intact roots of *Halophila ovalis* as a function of distance behind the root tip and shoot illumination. *Aquat. Bot.* **1999**, *63*, 219–228. [CrossRef]

76. Greve, T.M.; Borum, J.; Pedersen, O. Meristematic oxygen variability in eelgrass (*Zostera marina*). *Limnol. Oceanogr.* **2003**, *48*, 210–216. [CrossRef]